Published in final edited form as:
J Struct Biol. 2011 May ; 174(2): 400–412. doi:10.1016/j.jsb.2011.01.005.

Retrofit implementation of Zernike phase plate imaging for cryo-TEM

Michael Marko[1], **ArDean Leith**[1], **Chyongere Hsieh**[1], and **Radostin Danev**[2]

[1]Resource for Visualization of Biological Complexity, Wadsworth Center, New York State Department of Health, Empire State Plaza, Albany, NY 12201-0509, USA

[2]Okazaki Institute for Integrative Bioscience, National Institutes of Natural Sciences, 5-1 Higashiyama, Miyodaiji-cho, Okazaki, Aichi 444-8787, Japan

Abstract

In-focus phase-plate imaging is particularly beneficial for cryo-TEM because it offers a substantial overall increase in image contrast, without an electron dose penalty, and it simplifies image interpretation. We show how phase-plate cryo-TEM can be implemented with an appropriate existing TEM, and provide a basic practical introduction to use of thin-film (carbon) phase plates. We point out potential pitfalls of phase-plate operation, and discuss solutions. We provide information on evaluating a particular TEM for its suitability.

Keywords

Zernike phase plate; cryo-EM; contrast-transfer function; EM automation

1. Introduction

1.1 Development and types of phase plate

In the TEM, a phase plate is placed at the objective lens back focal plane, which is the objective aperture position and also the diffraction plane. Its function is to shift the phase of electrons scattered by the specimen relative to that of the unscattered beam. Thus, phase contrast is generated when the objective lens is close to focus, thereby avoiding the oscillations in the contrast-transfer function that arise in conventional phase-contrast imaging using underfocus. A very old idea (Boersch, 1947), various types of phase plates have been tried in the past, making for interesting reading. Examples are (Kanaya et al., 1958; Faget et al., 1962, Möllenstedt et al., 1968; Badde and Reimer, 1970; Thon and Willasch, 1970; Toguchi et al., 1970; Hoppe, 1971; Unwin, 1971, 1973; Krakow and Siegel, 1975; Balossier and Bonnet, 1981), and include a report by the precursor of the Albany lab (Johnson and Parsons, 1973). However, it has only been recently that TEM technology has advanced sufficiently to make phase-plate use practical.

Corresponding author: Michael Marko, Wadsworth Center, P.O. Box 509, Empire State Plaza, Albany, NY 12201-0509, USA, marko@wadsworth.org, Tel +1 518 474 7049, Fax +1 518 408 1815.

The renaissance of phase plates in the Nagayama lab at Okazaki (Danev and Nagayama, 2001; reviewed in Nagayama and Danev, 2008; Danev and Nagayama, 2010) has led to the efforts currently underway in a few laboratories worldwide. Phase-plate development has been the major focus of the Okazaki lab since 1999, and was taken up at Albany starting in 2003 (Marko et al., 2005, 2007, 2010), but at a much lower activity level until recently. The other laboratories working on phase-plate development are mentioned below. Practical use has been demonstrated for single-particle reconstruction (Danev and Nagayama, 2008; Yamaguchi et al, 2008, Shigematsu et al., 2010), cryo-tomography (Danev et al., 2010, Hosogi et al., 2010), and in both of these as well as electron crystallography (Murata et al., 2010).

There are two major types of phase plate currently being tested. The continuous-film type is the only one that is immediately suitable for practical use in biological cryo-EM. This type consists of a 10-to-30-nm-thick film (usually of carbon) placed over the objective aperture. A small central hole is made in the film. The unscattered electrons pass through the hole, while electrons scattered by the specimen pass through the carbon film. The thickness of the carbon film is chosen such that its inner electrostatic potential shifts the phase of the electrons by $\pi/2$ or 90°, at the particular accelerating voltage in use. Scattering in the film can reduce the contrast gain by 20%, but this effect can be largely overcome by using a thinner phase plate and a small amount of defocus. A detailed report on the use of carbon-film phase plates is provided in Danev et al. (2009), and an excellent review concentrating on their practical use is presented by Danev and Nagayama (2010). These should be read by anyone contemplating use of phase-plate imaging.

There are a few variants of the continuous-film type. With a half-film type, known as the Hilbert phase plate (Nagayama 2002; Kaneko et al, 2006; Setou et al., 2006; Barton et al., 2008), the edge of a film is brought close to the unscattered beam in the back focal plane (the film in this case is made to provide a phase shift of π). Thus, only electrons in one side of the diffraction plane are scattered by the specimen and are phase-shifted. This gives strong asymmetric contrast similar in appearance to differential-interference contrast in light microscopy. When using a Hilbert phase plate, the unscattered beam can be placed in an arbitrary position relative to the edge of the film, which could result in improved phase-contrast transfer of information at lower spatial frequencies.

However, because of the asymmetric contrast, images recorded with a Hilbert phase plate must be computationally corrected to yield results equivalent to a Zernike phase plate before image-processing for 3-D reconstruction. By A further variant of the continuous-film type is to use a very thin film with no hole, which is locally charged by the unscattered beam to produce a phase shift (Malac et al., 2010).

The other major type of phase plate employs a microfabricated device in the back focal plane to create a uniform electrostatic (Matsumoto and Tomomura, 1996; Majorovits and Schröder, 2002) or magnetic (Nagayama et al., 2008) field to create the phase shift. An electrostatic phase plate would be ideal for tomographic tilt-series recording of thick specimens, because the phase shift could be adjusted according to the tilt angle. This would take into account the increasing phase shift of the specimen itself, as its effective thickness increases, and would accommodate specimens of widely varying thickness. The same phase plate could also be used at different accelerating voltages.

Electrostatic phase plates of the einzel-lens type (Majorovits et al., 2007; Huang et al., 2006), or the drift-tube type (Cambie et al., 2007), have a central element that shifts the phase of the unscattered electrons. The structure of the central element, and its supporting wire(s), blocks information transfer, especially at low spatial frequencies. Although progress

is being made to reduce the size of the central element (Chen et al., 2008; Shiue et al., 2009, Alloyeau et al., 2010), the current remedy for excessive low-frequency blocking is to use a modified TEM that has one or more extra lenses to magnify the diffraction plane where the phase plate is inserted (e.g. Majorovits et al., 2010). This ameliorates problems with extreme miniaturization of the electrostatic element.

Although still having a supporting wire, the “Zach phase plate” (Schultheiss et al., 2010) produces an electrostatic field at the end of the cantilevered support, and has no central obstruction. An alternate proposal is the “anamorphotic” electrostatic phase plate, which has no blocking elements. While this may be the ideal phase plate, it must be placed within a multipole lens system, such as is used in an aberration corrector (Schröder et al., 2007; Frindt et al, 2010). An even more recent concept uses a high-energy photon beam focused on the unscattered electron beam to shift its phase by the “ponderomotive force” (Müller et al., 2010).

1.2 Contrast enhancement

The vitreously frozen samples used for cryo-TEM tomography and single-particle reconstruction consist mostly of low-Z elements. Consequently, the number of electrons scattered to high angles is low, resulting in very little amplitude contrast, and requiring imaging by phase contrast. In conventional imaging of these specimens, phase contrast is achieved by using strong objective-lens undefocus. This results in an oscillating contrast-transfer function (CTF). Maximum information transfer only occurs at the peaks of this function. At certain spatial frequencies there is zero transfer, and at others the transfer is with reversed contrast. With a phase plate, images can be recorded in-focus, with high contrast, and near-maximum contrast is maintained over a broad range of spatial frequencies. The overall contrast increase is about two times, but as shown in Danev et al. (2009), it can be much greater at certain (especially lower) spatial frequencies.

In conventional TEMs, phase contrast comes only from elastically scattered electrons. Thus, to achieve optimum results for either conventional underfocus imaging or near-focus phase plate imaging, zero-loss energy filtering should be used to remove the inelastically scattered electrons. Because of chromatic aberration, inelastically scattered electrons are not in focus at the image plane, and effectively add only noise to the image. If the proportion of elastic scattering is small compared to inelastic scattering, phase plate imaging will have little effect on contrast improvement. Nevertheless, it is important to point out that the functions of the phase plate and the energy filter are independent; an energy filter is not required to obtain the benefits of phase-plate imaging.

1.3 Simplified image interpretation

The relationship between mass (i.e. scattering) in the specimen and image intensity is modulated by the CTF. When using high-underfocus imaging, the transfer of information greatly varies with spatial frequency. CTF correction, and the use of focal series of images, can address this problem, although these techniques are generally impractical for cryo-tomography. With a proper set-up, near-focus phase-plate imaging can provide constant, near-maximum, transfer of information over the range of spatial frequencies of interest in tomographic or single-particle cryo-TEM (e.g. 0.5 - 40 nm). Furthermore, with phase-plate imaging, the focus gradient of a tilted specimen does not have a significant effect on the CTF for a resolution of 1 - 2 nm (Danev et al., 2009). Thus, when analyzing the 3-D reconstruction, the CTF does not need to be considered when seeking to establish a relationship between voxel intensity and mass at the corresponding point in the specimen.

2. Methods

2.1 Phase plate manufacture

We describe here the methods used at Albany, which differ somewhat from those used at Okazaki. Only thin-film phase plates will be considered, since a modified TEM would be needed in order to effectively use microfabricated electrostatic phase plates, and also because a typical TEM lab is not equipped to manufacture the latter.

Phase plates are made by picking up carbon films on 2-mm-diameter Pt disks, each having a linear set of nine aperture holes, 50 μm in diameter. These disks fit the standard objective aperture holder of our JEOL JEM-4000FX. Strips, or disks of any diameter, with any pattern of aperture holes, are available as a custom order from Ladd Research (Williston, VT).

For an accelerating voltage of 400 kV, we use a carbon film thickness of 32 nm. We measure the thickness by TEM observation of the curled edge of a broken film, and also by optical densitometry of the carbon film evaporated on a glass slide (Moretz et al., 1968). The two methods agree well. The carbon film thicknesses for a $\pi/2$ phase shift are 27 nm for 200 kV, 31 nm for 300 kV, and 33 mm for 400 kV, but somewhat thinner films are usually preferable (Danev et al., 2009). Electron-energy-loss spectroscopy can be used to measure the phase plate thickness, while the phase plate is place in the back focal plane, although this gives an underestimate of the phase plate thickness, due to an inappropriate collection angle. Nevertheless, the technique is useful for monitoring any increase in thickness.

We use 1/8-inch diameter, spectroscopically pure, pre-sharpened carbon rods (cat. no. 12420, E.F. Fullam, Clifton Park, NY – now available from Ted Pella, Redding, CA). We evaporate carbon on freshly-cleaved mica with an oil-free Bal-Tec MED-20 vacuum evaporator (Leica Microsystems, Vienna). Several runs are needed to build up the desired thickness. We then float the carbon onto distilled water and pick up small pieces of the film on the aperture disks. Transfer of the carbon film from mica to the aperture disk is a likely source of contamination and variability in quality among phase plates. Careful note of the details of this procedure should be taken, and correlated with phase-plate quality to find the optimal procedure.

We mount all the disks in the (detachable) aperture holder blade, and then make a central hole in each aperture using a focused ion beam / scanning electron microscope (FIB/SEM) instrument (Nova V-600, FEI Co., Hillsboro, OR). We use a 30 keV Ga^+ ion beam at a current of 12 pA for imaging (by detection of secondary electrons), and a beam current of 2.8 nA for cutting the hole. In each aperture, we pattern a 0.7 μm diameter circle for 10 sec. Due to alignment differences between beam current steps, the actual hole size may be larger or smaller than the circle drawn on the low-current image, thus the hole-size ratio has to be experimentally determined. The FIB procedure is not time-consuming and, as in our case, it can be done using a FIB in a nearby institution's materials science lab.

It is essential that the carbon film be free of contaminants. We believe that it is important that both the carbon evaporator and the FIB or FIB/SEM have oil-free vacuum systems. We find that it is helpful to plasma-clean the entire aperture holder blade within an hour before inserting it into the TEM. We clean for 40 seconds with 25% oxygen in argon in a Model 1020 plasma cleaner (Fishione Instruments, Export, PA). Using these precautions, we find that the "wrapping" technique described in Danev et al. (2009) is not needed. Note that this treatment reduces the carbon-film thickness by about 5 nm, and this should be taken into account when preparing the film.

We are starting work on a design for thin-film Zernike phase plates that would enable them to be mass-produced by microfabrication techniques, and made available at low cost. Hilbert (half-film) phase plates do not require the central hole, thus they are easier to fabricate. However we believe that Zernike phase plates are simpler to use, and they have the advantage that the images can used directly for 3-D reconstruction.

2.2 Determination of the proper cut-on frequency

The "cut-on" frequency of a carbon-film phase plate is the spatial frequency below which information is not transferred by phase contrast. For convenience, we will express this as a cut-on spacing (d). The cut-on spacing is determined by the accelerating voltage (expressed as wavelength, λ), the focal length of the objective lens (f), and the radius of the central hole in the phase plate (r) by the simple relationship $d=f(\lambda/r)$.

Thus, to determine how a given TEM can be used for phase-plate work, one must consider what the lowest phase-shifted spacing should be for a particular specimen or experiment. According to Danev et al. (2009), in the case of single-particle work, the cut-on spacing should be twice the particle size. However, in the case of cellular tomography, where particles are not isolated on a uniform background, and where structures of many sizes are present, one may simply consider the cut-on as representing the largest spacing that will be phase-shifted. In the case of cellular tomography at 2-4 nm resolution, we believe that a cut-on spacing of 20 nm is sufficient, and even smaller spacings are useful, especially if contrast of membrane profiles is the major interest.

Figure 1 shows the cut-on spacing for 200, 300, and 400 kV as a function of focal length, for both 0.3- and 0.7-μm diameter phase-plate hole sizes. The minimum practical hole size for an FEG TEM is about 0.3 μm, while it is about 0.7 μm for LaB_6 instruments.

In the examples shown here, we used a JEOL JEM-4000FX with a focal length of 3.1 mm, an accelerating voltage of 400 kV, and phase-plate central-hole diameters of about 0.7 nm, giving cut-on spacings of only 14-16 nm. Although this is far from optimal, we nevertheless obtained significant contrast improvement.

2.3 Modification of the objective aperture holder

The key requirements for an aperture holder for phase-plate use are that the phase plate central hole has to be kept centered on the unscattered beam, and the phase plate has to remain free of contamination that causes charging. With most standard aperture holders, it is difficult to keep a sub-micron hole centered manually. Although fine centering can be done using the condenser tilt deflectors (see 2.10 below), and this is perfectly acceptable for occasional single images, for automated collection of a series of images it is desirable to add mechanical fine centering that can be computer-controlled.

As shown in Figure 2, we added piezo drivers (MICI-140, Piezosystems Jena, Jena, Germany) to the standard objective aperture drive of our JEOL JEM-4000FX. In the direction along the axis of the holder, the driver simply works against the column vacuum, in series with the manual adjustment. The left-right movement is accommodated by slightly compressing the o-ring on the aperture holder mounting flange. A thin plastic pivot is provided for this purpose, along with springs that exert a force considerably greater than that needed to compress the o-ring. Thus, the piezo driver rocks the aperture holder left and right against the spring tension. Control of this system is described in section 2.10, below.

In most TEMs, contamination rapidly builds up on the phase plate when in use, resulting in a short useful lifetime. This can be avoided by heating the phase plate. In some cases, the temperature is set as high as 250°C, and heating is done even when the TEM is idle. Thus

ideally, the aperture holder should be fitted with a heater, as described in Danev et al. (2009). However, it has been noted that phase-plate contamination may not be not a problem if the TEM has an oil-free vacuum system (R. Schröder, personal communication). In the case of our JEM-4000FX (which does not have an oil-free vacuum system), we do not heat the phase plate, and we do not experience sufficient contamination to preclude practical use of phase plates. This may be due to the very narrow clearance (about 0.5 mm) between the phase plate and the anticontaminator above it, and the lower objective polepiece below it. The fact that we never use photographic film may also contribute to a clean vacuum system. Our recommendation for new users is to first try a phase plate in the standard objective aperture holder before undertaking modifications.

2.4 TEM alignment

Alignment of the TEM is more critical for phase-plate use than for general cryo-EM imaging, although the phase-plate conditions are in fact also optimal for general imaging. In order that the unscattered beam passes completely though the central hole in the phase plate, the final condenser lens, should be set for parallel illumination at the specimen level. This is also the proper condition for electron diffraction, giving a minimum size (crossover) of the unscattered beam at the back focal plane, where the phase plate is located. This is called the “on-plane” phase-plate condition. However, in many electron microscopes, parallel illumination at the specimen would place the illumination crossover within the lower objective polepiece. Thus, the illumination angle at the specimen may have to be compromised in order to place the crossover in the plane of the objective aperture (phase plate).

When a phase plate is installed, the proper setting of the final condenser lens can be found by observing the image of the phase plate central hole, which may be very small at first. The condenser lens excitation is varied to make the image of the hole larger. At some point, the image of the central hole will fill the field, and while continuing to varying the condenser lens it will get smaller again. The condenser lens is properly set when the image of the hole fills the field. This sequence is shown in Figure 3.

As a check, if a phase plate is not yet installed, or to check the suitability of a TEM for phase-plate use, the parallel-illumination condition can be roughly confirmed by varying the objective lens excitation over a wide range, and noting that the size of the illuminated area does not change. The diffraction pattern should be approximately in focus under this illumination condition.

When a tilting experiment is to be done (e.g. collection of a tomographic tilt series), a check should be made that the illuminated area should not significantly change in size or position over the focus range needed, otherwise phase-plate imaging may be impractical. If, with a particular TEM, the focus change during tilting is more than about 10 μm, an illumination-center alignment may be needed to avoid illumination shift. This will slightly mis-align the TEM with respect to the voltage and current centers, and will certainly preclude coma-free alignment; however this mis-alignment should be tolerable for most tomography applications. The illumination alignment is done by wobbling (or manually varying) the objective lens and adjusting the condenser-tilt deflectors for minimum movement of the illuminated area on the specimen, while re-centering the illumination with the condenser-shift deflectors. If necessary, the tilt-purity alignment should first be touched up so that excessive beam shift does not accompany beam tilt.

Good practice dictates that the beam should be as coherent as possible. It is best to use the smallest spot size setting (upper condenser lens) that gives adequate illumination intensity, with a relatively large condenser aperture if necessary. Generally, in order to maintain

parallel illumination, the intensity can be varied only by upper condenser lenses and the beam current, while the size of the illuminated area can be varied only by choice of a condenser aperture. However, when there is a condenser lens below the condenser aperture (e.g. a condenser minilens), both the size and the intensity of the illuminated area can be varied while maintaining parallel illumination.

In the case of FEI TEMs, which are normally operated in the “Microprobe” mode, parallel illumination may not be bright enough at higher magnification. In this case, it may be necessary to use the “Nanoprobe” mode when setting up parallel illumination.

Once the set-up and alignment for phase plate imaging is completed, save the values of the condenser lenses, and the x-y values of the condenser tilt and shift deflectors, so that they can be recalled as needed (see sections 2.8 and 2.9). Most modern TEMs provide a way to store and recall lens and deflector settings; otherwise they should be manually recorded.

2.5 Beam-blanker testing

An above-the-specimen beam blanker is always used for low-dose cryo-EM work. Because it is essential to keep the unscattered beam centered in the phase-plate central hole, the beam must come back to exactly the same place after blanking. To test this, observe a small beam spot at high mignfication (100 kX or more). To avoid any confusion from charging of the aperture or specimen, do this with no specimen, and with the objective aperture retracted.

The beam blanker (“alternate shutter”) function provided with most CCD cameras acts by introducing a deflection of the beam at the electron gun, through control of one of the gun alignment deflector coils. If the beam (i.e. the crossover spot) does not always come back to the same position when using the CCD camera’s beam-blank method, try using the EM controls directly for beam blanking (this is usually part of the built-in low-dose imaging function intended for recording on photographic film). This will reveal if the problem is due to hysteresis of the deflector coil or charging in the upper column. Most likely, there will be no problem with direct EM control. The problem will more likely be due to the connection between the CCD camera control unit and the TEM. This connection should be done via an optocoupler. The camera manufacturer should be contacted to be sure there is a properly-isolated connection to the TEM, but most likely the problem will remain because the “contact resistance” of the optocoupler (solid-state relay) varies with the input from the camera controller, which may not be sufficiently constant. We experienced this problem with our Gatan MSC 794 camera and JEM-4000FX TEM, and we solved it by using the internal EM control (as used in the internal “MDS” function) to perform the beam-blanking.

To avoid unnecessary exposure of the specimen, the beam should remain blanked except when needed. It is very convenient to install a foot pedal to unblank the beam, especially when using the “robust low-dose method” described in Section 2.9. If the CCD camera controller’s beam-blank function is adequate, a similar method can be used here. Any foot-pedal switch can be used. The foot pedal turns on a power supply that provides input to a normally closed solid-state relay (e.g. Crydom DO061A-B, Digi-Key, Thief River Falls, NM). The relay is placed in the low-voltage DC control line between the camera control unit and the TEM. A mechanical relay is not suitable because the contact resistance may vary. However, as mentioned above, the contact resistance of the solid-state relay can vary if the footswitch contact resistance varies, so the solid-state relay for the foot pedal has to be activated by switching the power supply, not by directly interrupting the DC input voltage with the footswitch. Footswitch operation of the beam blanker can alternately be accomplished via the TEMs internal beam-banking function by connecting the footswitch in parallel with a microswitch in the computer mouse, and that is the method we use.

2.6 Phase plate testing

When developing the protocol for making phase plates, it is necessary to check the phase shift to ensure that the film thickness is appropriate. In routine use, it is necessary to check the quality of each phase plate each time it is used.

2.6.1 Determination of phase shift—The proper phase shift can be determined by using the phase plate in imaging a thick (about 20 nm) amorphous-carbon-film specimen with a few micrometers of underfocus, and then with same amount of overfocus. When observing the power spectra, the spatial frequency of the first CTF zero should be the same in both cases, if the phase shift is $\pi/2$. Note that the in-focus setting should be determined by the power spectrum (as in Figure 4), and not by the image wobbler. The in-focus power spectrum is characterized by no visible minima and a smooth fall-off in intensity from the origin. However, as mentioned in Danev et al. (2009), it is often desirable to use a phase plate with less than $\pi/2$ phase shift. In this case, the positions of the CTF zeros at a relatively high underfocus can be fitted to a computed phase-plate CTF. This test should be done when the phase-plate is newly inserted, before it becomes charged (see below). Once the relationship between film thickness and phase shift is confirmed, it is not necessary to check the phase shift again, except to compensate for charging.

2.6.2 Testing and compensation for charging—As described in Danev et al. (2009), phase plates may work well at first, but they deteriorate over time. The deterioration manifests itself by charging of the phase plate. The charge can act as an electrostatic lens and change the focus relative to the wobbler pivot point. A mild amount of charge can be compensated by over- or under-focusing. It practice, it is rare that the focus with phase plate is the same as wobbler focus. This is important for automated data-collection systems that use auto-focus based on image shift induced by beam tilt; it is necessary to determine the offset between wobble (beam-tilt) focus and focus with the phase plate inserted.

Charging is easily assessed by recording an image of an amorphous film at relatively high defocus. An indication of charging is a CTF minimum appearing close to the origin, as shown in Figure 5. This first minimum may be much narrower than those at higher spatial frequency. When a lower defocus is used with the same phase plate, this narrow, low-frequency first minimum is widely separated from those at higher frequency. This “false” first minimum is not used for determining a defocus offset. The true first minimum, which correlates with the focus offset needed to compensate for charging, is the next higher in frequency. A further indication of charging, as seen in the CTF, is that the higher-frequency zero-crossings do not match up with the calculated CTF (Fig. 5). This effect was first described in Danov et al. (2001).

Gross contamination on the phase plate can be seen when imaging the phase plate directly. With many TEMs, it is possible to bring the phase plate into focus by using the low-magnification mode (objective lens off or weak, e.g. Figure. 6D). If no trace of contamination is observed on the phase plate, yet it does not behave as expected, it may have acquired an excessive overall charge, likely due to the presence of a thin insulating layer. The presence of such an insulting layer may be evidenced by a small oxygen edge (of uncertain origin) in the EELS spectrum of a phase plate (Fig. 7).

2.6.3 Testing for tendency to charge—Although it is not necessary to perform this test routinely, when initially developing one’s own protocol for making phase plates, the tendency to charge can be assessed by the “Berriman effect” (Brink et al., 1998; Downing and Glaeser, 2004; Downing et al., 2004), as shown in Figure 6. The Berriman effect is a “footprint” imprinted on a carbon film as a result of moderate electron irradiation (Fig. 6A).

The footprint represents locally altered charge induced by the beam, which is made visible at very high defocus because of a relative phase shift. The footprint will be light if the charge is positive (the usual case), and the condenser lens is highly overfocused relative to the "on plane" condition. The footprint can be made dark by underfocusing the condenser lens. If a similar irradiation is made on a different part of the carbon film, the first footprint will be at least partly erased, and the most recent one will be visible.

With no specimen under the beam, insert the phase plate and set up the "on-plane condition" as described in Section 2.4. Blank the beam, set one of the condenser tilt deflectors to an amount several times greater than that used to accomplish fine centering of the phase plate, and note the setting. Make an exposure with an electron dose typical for recording an image, 100-1000 e^{-}/nm^{2} at the specimen plane for a 1-nm pixel size. The electron dose in the small spot on the phase plate will be four orders of magnitude higher. The image need not be saved; the purpose is to irradiate the carbon film adjacent to the central hole. Note the setting of the final condenser lens, and increase the lens current by 10-15%; this will reduce the electron flux on the phase plate to well below 1 $e^{-}/nm^{2}/sec$ and set the "off-plane" condition, making the phase-plate central hole visible.

Record an image, which should show a small shadow of the central hole (if the shadow is too large, use a higher condenser-lens current). Carefully inspect this image. Most likely, there will be a faint spot, somewhat smaller than the central-hole shadow, somewhere on the carbon film, as shown in Figure 6A. If no spot is visible, the phase plate is free of charge. If a spot is visible, to confirm the Berriman effect, return the condenser lens and condenser tilt deflector to the original settings, and then irradiate a different area of the carbon film (by using a different condenser tilt setting). The original spot should be weaker, and the new spot should be visible. A side-benefit of this procedure is that it shows the size of the unscattered beam relative to the size of the phase-plate central hole, when the condenser lens is set to the on-plane condition.

It may be possible to at least partially "burn off" the charge on the phase plate (as shown Fig 6E-H) by reducing the magnification and using a large condenser aperture and high beam current to strongly irradiate the whole carbon film. This may neutralize the charge and/or remove the thin insulating layer of contamination that supports the charge.

2.7 Focusing with the phase plate in place

As already mentioned, since phase plates nearly always are at least slightly charged, the image wobbler or beam-tilt methods cannot be directly used to find focus. It will be necessary to observe a "live" power spectrum, using a CCD camera operating with a rapid refresh rate. An example of focus on a typical specimen, using a relatively charge-free phase plate is shown in Figure 4. The most reliable way to reach focus is to iterate between over- and underfocus, as seen by the Thon rings, and find the midpoint. We recommend use of a pixel size on the specimen that is about one-quarter of the target resolution, and the focus should be adjusted so that the intensity fall-off in the power spectrum is just beyond the twice-Nyquist frequency of the CCD camera.

2.8 Use of a conventional low-dose imaging method for tilt-series collection

If the specimen does not need to be tilted, or if the objective lens focus range needed to record a tomographic tilt series is not more than a few micrometers, a standard low-dose tomography protocol can be used, with some modification of the off-axis "Focus" step to include phase-plate centering.

To test the suitability of a TEM for this method, set up the Exposure position for the proper phase-plate illumination conditions. Set up the Focus position at the same magnification,

off-axis along the tilt axis, and then defocus the condenser lens so that the shadow of the phase plate central hole is visible. Both condenser-shift and condenser-tilt deflectors will be needed in order to center both the illumination and the phase plate central hole.

Mechanically shift the phase plate position by a small amount. Note the x and y values of the condenser tilt, and then adjust the condenser tilt deflectors to center the phase plate central hole. Record the Δx and Δy deflector values. Recall the Exposure position and apply the same Δx and Δy values to the condenser tilt in the exposure position. Slightly defocus the condenser and confirm that the phase-plate hole is centered. If this works over the whole focus range needed for the data-collection protocol, the existing low-dose imaging software can be modified accordingly.

However, if the condenser-tilt Δx and Δy values determined in Focus become incorrect for Exposure as the objective focus is reset as needed for high-tilt images, it will be necessary to use the alternate, more robust method below.

2.9 Use of a robust low-dose imaging method for tilting data collection

In this method, all operations (e.g Search, Focus, Exposure) are done on-axis. Thus, the specimen receives additional irradiation beyond that strictly necessary to record the tilt image. To minimize this dose overhead, a lower magnification is used for positions other than Exposure. A camera with a frame rate of about 30 per second is needed, and this will often mean that two cameras will be used, a low-resolution fast camera for focus and centering, and a high-resolution camera for collecting the final images.

For the moderate resolution expected in most cryo-tomography work (3-4 nm), phase plate imaging affords a rather wide focus tolerance, about 2 μm (Danev et al, 2009). This not only avoids problems with tilted specimens, but it also means that lower-magnification focusing with an image wobbler (using appropriate additional offset for phase-plate charging) is adequate. We have found that the focusing magnification can be ten times lower than the exposure magnification, resulting in a dose rate 100 times lower (Typically 50 $e^{-}/nm^{2}/sec$ for Exposure and 0.5 $e^{-}/nm^{2}/sec$ for Search). Accurate centering of the phase plate can be done at an even lower magnification, twenty times lower than the Exposure magnification (typically 0.13 $e^{-}/nm^{2}/sec$).

We have implemented a simple, robust semi-automated data-collection scheme for use with our JOEL JEM-4000FX TEM. This was necessary because the focus change over the entire tilt range is so great that the correspondence between off-axis and on-axis phase plate center is not maintained, and also because a specimen feature cannot be tracked within the range of electronic image shift. We therefore currently carry out feature centering, focusing, and phase-plate centering manually.

This scheme is presented as a “case history” example. Although our use of a post-column energy filter and two cameras is not typical, the principles are not specific to JEOL TEMs except as noted.

Figure 8 shows the user interface for our data collection scheme, which provides for tomographic tilt-series collection or single-shot imaging.

In the Exposure mode, we record the image with the 2K CCD camera of our post-column energy filter (GIF2002, Gatan, Pleasanton, CA). Our user interface passes commands to Gatan Digital Micrograph for recording the images in a file series. In the Search mode, we use a near-axis TV-rate camera (F-114, TVIPS, Gauting, Germany). The difference in magnification between these cameras is partly due to the high post-magnfication of the GIF

CCD, and is also determined by custom settings of the intermediate lenses, resulting in a magnification difference of ten times. In the phase-plate Center mode, the magnification difference is about 20 times. In this case, the intermediate lenses are kept at the same values as set in the Exposure mode, and the magnification difference is due solely to the difference in post-magnification of the two cameras.

Centering of the object is done in the Search mode with the mechanical stage drives, avoiding any change in the electron optics due to image shift. Focusing is done using the image wobbler in the Search mode. The objective lens value thus determined is automatically applied when in the Exposure mode, and any defocus needed to compensate for phase-plate charge is included. A correction is automatically applied via the Spectrum Offset function of the GIF, in order to keep the slit centered on the zero-loss peak (a large change in the objective lens current causes the zero-loss peak to shift significantly).

In the phase-plate Center mode, all EM settings are identical to the Exposure mode except for: (1) the projector lens deflectors, needed to move the image center to the off-axis TV-rate camera position, (2) the gun tilt, used to lower the illumination intensity to the minimum needed, without making any change in the condenser lens system, and (3) the final condenser lens, which is adjusted away from the “in-plane” condition in order to make the phase-plate central hole visible. In the Center mode, the phase plate is centered by a slight adjustment of the condenser shift deflectors. Fortuitously, because there is a small amount of residual condenser tilt associated with condenser shift (i.e. the “shift purity” is cannot be made perfect), if we use the condenser shift deflectors to re-center the phase plate central hole, the illumination is also re-centered on the CCD camera. We have found this to be the case with most JEOL TEMs. With other TEMs, it may be necessary to use the condenser shift deflectors to center the illumination and the condenser tilt deflectors to center the phase plate.

Switching between the three positions is very fast, in spite of a slow serial interface to the EM internal computer, because we make use of the JEOL’s internal “UFC” memories rather than issuing a long series of commands for individual lenses and deflectors. Many FEI TEMs, and newer JEOL TEMs, have a fast external-control interface, and individual commands to set lenses and deflectors can be used, or an existing external low-dose imaging system (such as one intended for tilt-series collection) can be modified according to the general scheme presented here. Our GUI is written as a webpage using Java script, and we will gladly provide the script (useable for older JEOL TEMs: 1200, 2000, 3000, 4000 series), as well as advice for implementing phase-plate imaging.

2.10 Phase plate centering

Ideally, the phase plate should be centered by mechanical means only, so that there is no alteration of the electron-optical set-up during phase-plate imaging. In any case, mechanical centering is essential for the initial set-up, so that the phase plate central hole initially does not shift when the condenser lens current is varied.

Figure 9 shows our interface for piezo fine-centering. Several corrections are incorporated. Because the translation is done differently for each axis (see Fig. 2), the displacement of the phase plate for a given applied piezo voltage, and the amount of backlash to be accommodated, is different for the two axes. In addition, the movement of the phase plate has to correspond to the displayed image from the TV-rate camera, so that the user can easily judge the direction in which the phase plate must be moved. There are two modes for centering the phase plate: orthogonal x-y movement (with three choices of step size), and one-step movement in the desired direction, and by a desired amount, using the target.

Although our centering system is capable of 10-nm precision, iteration is needed to reach the desired position, and we find that it is faster to do the fine centering using the condenser-tilt deflectors, as described above. For medium-resolution (~2 nm) microscopy, the misalignment due to this small condenser deflection is inconsequential, however, as we seek higher resolution, we will seek to improve the mechanical centering. In principle, the location of the phase plate central hole can be found by image-processing, and automatic phase-plate centering should be possible. A precision of 20 nm should be adequate, even with phase-plate central holes of 300-nm diameter. A much-improved phase-plate holder is under development with collaboration with Hummingbird Scientific (Lacey, WA), who plan to make it commercially available. We expect that such a capability will be also be provided for future JEOL phase-plate TEMs

Since current carbon-film phase plates do not have a long life, it is very beneficial to equip the phase-plate holder with an airlock so that phase plates can be changed as easily as a specimen, without the need to warm the TEM stage or anticontaminators, or to vent the column. This has already been implemented for certain JEOL TEMs (Shiue et al., 2010 Motoki et al, 2010).

2.11 Image-series recording

As an example of implementation on a particular TEM, the following is our procedure for phase-plate imaging on the JEM-4000FX. Please refer to Figure. 7. The same interface can be used for either tilt series collection or for a series of single images (by setting a tilt increment of zero). Although this protocol is specific in detail to our particular TEM and accessories, the basic scheme is not microscope-specific.

1. Set the objective lens current to the previously determined eucentric focus value.
2. Focus the specimen with the mechanical z-height control.
3. Select the *Pixel size, Tilt increment, Next tilt angle* (zero for single images), filename template, *Next image number*, and *Exposure time*.
4. Recall the lens and deflector settings, after alignment as described in Section 2.4.
5. Center the illumination, and load the x and y condenser-shift deflector settings into the *Con shift* boxes using the *Read* button. If, during the tilt series, it becomes necessary to mechanically move the phase plate, the condenser shift deflectors should first be returned to these initial settings, using the *Set* button.
6. Insert and center the phase plate mechanically, with the aid of the piezo drives.
7. Center the phase plate with the condenser-tilt deflectors and *Read* the deflector values into the *Con tilt* boxes.
8. Be sure the final condenser is set for the “on-plane” condition (maximized size of the shadow of the phase-plate central hole).
9. Focus the image with the wobbler and the record power spectrum.
10. If the power spectrum shows evidence of defocus (due to charging of the carbon film), find the focus difference between wobble-focus and true focus and enter it in the *Defocus (nm)* box.
11. For a tilting experiment, tilt the specimen to the maximum tilt to be used, and refocus the image.
12. Re-center the phase plate with the x and y condenser shift deflectors.
13. Select PP *Search*.

14. Mechanically re-center the image and re-focus the objective lens. The wobble focus should be correct within +/− 0.5 μm for a 1-nm pixel size on the specimen. Any additional focus increment will be automatically applied. The final focus value is passed to the PP *Center* and PP *Exposure* positions.
15. Select PP *Center*. Viewing with the TV-rate camera, re-center the phase plate central hole, using the condenser shift deflectors.
16. The incremental condenser shift values are passed on to the PP *Exposure* position.
17. Select PP Exposure. Record the image. The energy-selecting slit is automatically re-centered according a focus-offset table, but an additional correction can be added in the eV offset box if there is energy drift.
18. Acquire the image with the *Acquire* button. If the phase plate is not centered, go back to PP *Center*, then use PP *Exposure* again.
19. Save the image and go to the next by pressing the *Next* button. If tilting, this will cause the stage to be tilted according to the chosen *Tilt increment*.

2.12 Preparation of the test specimen

Rat liver tissue was high-pressure frozen (Bal-Tec HPM-010, Leica Microsystems, Vienna), and vitreously frozen sections were prepared by cryo-ultramicrotomy (UCT/EM-FSC, Leica Microsystems, Vienna). The sections were prepared in 2005, as described earlier (Hsieh et al, 2006). The section thickness was 200 nm.

3. Results and Discussion

3.1 Comparison of phase-plate and high-underfocus imaging

We documented the contrast improvement due to near-focus phase-plate imaging by a simple comparison of 2-D images. To better show the difference in contrast, we used an electron dose of $1000e^{-}/nm^{2}$ for each of these images, rather than less than $100e^{-}/nm^{2}$, as would be used for a tomographic tilt-series image. Figure 10 clearly shows the increased contrast of phase-plate imaging compared to high-underfocus imaging, both visually and by comparison of plots of the rotationally averaged power spectra. According to Danev et al. (2009), our cut-on frequency of 14 nm was far from optimal, yet the contrast improvement is significant. Although the overall contrast gain would be expected to be considerably higher with a lower cut-on frequency, the membrane profiles and other fine features are of greatest interest in this case, and the increased membrane contrast is shown by the plots in the insets of Fig 10 C-D. Good contrast of a lipid-bilayer membrane, about 8 nm, is consistent with a cut-on spacing of 14 nm. For comparison, Fig 10D shows a conventional underfocus phase-contrast image, the CTF of which has a corresponding first-maximum spacing at 9 nm and a minimum (CTF zero) at 5.5 nm. Nearly identical results would be obtained with a 200- or 300-kV TEM, without energy filtering, given the same cut-on frequency and a specimen thickness not much greater than 0.5 inelastic mean-free path, or with thicker specimens if zero-loss energy filtering were available.

3.2 Summary and recommendations

We have shown that cryo-electron microscopy using a Zernike phase plate can be implemented on an existing cryo-TEM. We provided guidelines to determine if a particular TEM is suitable for phase-plate imaging, according to the focal length and accelerating voltage, and whether the TEM has a field-emission gun or not.

A simple, robust method was developed that was suitable even for an older TEM model that has poor goniometer eucentricity and simple computer control. The use of a lower magnification for focus, tracking, and phase-plate centering allowed these operations to be carried out manually and on-axis. Given such a TEM, a sensitive TV-rate camera is essential. The same camera, or preferably a second higher-resolution camera, could be used for recording the images. A simple EM control application is needed to switch the EM to the appropriate modes “Search”, Phase Plate Center”, and “Exposure”, and to control the camera(s) and any specimen tilting. This control system needs to transfer the objective lens value and the condenser deflector values from one mode to another.

For more modern TEMs that have a highly eucentric goniometer, and that use software for cryotomographic tilt-series collection (for example Serial EM; Mastronarde, 2005) or single-particle imaging (for example Leginon; Suloway et al., 2005 or JADAS; Zhang et al., 2009), the main modification that must be made to the software is to add phase-plate centering. Although the “modes” or “positions” need to be set up differently than for conventional cryo-TEM, the changes in lens and deflector settings can be accommodated without modification to the software. The primary required addition is to transfer the incremental condenser deflector settings determined in the “Focus’ mode (which will double as the phase-plate centering mode) to corresponding increments in the “Exposure” mode. The application will need to be run in the “semi-automated” mode, unless automatic phase-plate centering is implemented. Automated phase-plate centering, based on cross-correlation of images of the phase plate shadow in the Focus mode, should be possible given sufficient CCD-image contrast and adequate performance of the phase-plate centering mechanism.

The full benefit of phase plate imaging can be realized for thin specimens (e.g. 0.5 inelastic mean-free path) or with zero-loss energy filtering. When the image is dominated by inelastically scattered electrons, the “background” is already high compared to the phase-contrast signal, and the additional contrast due to phase-plate imaging does not have a great effect on the already-poor signal-to-noise ratio. The benefits of a phase plate for imaging dose-sensitive specimens has been analyzed in detail by Malac et al. (2008), where it was suggested that, when the resolution need not be better than 1 nm, there is no additional benefit to be gained from correction of spherical aberration. Thus, the combination of zero-loss energy filtering and phase-plate imaging should give the best possible results for cryo-EM imaging. Further improvement in low-dose imaging is therefore expected to come from better imaging detectors and reduction of beam-induced specimen movement.

In our opinion, the main challenges in phase-plate image collection at present are quality control of the phase plates themselves, and the performance of the fine-centering mechanism for the phase-plate holder.

Acknowledgments

We thank Kuniaki Nagayama of the Okazaki Institute for Integrative Bioscience for inspiring the project in the first place and for continual support since then. We thank Robert Glaeser and Dieter Typke of Lawrence Berkeley lab for many helpful discussions. We thank Kathy Dunn of the University at Albany College of Nanoscale Science and Engineering for use of the FIB and Michael Koonce of Wadsworth for the axoneme sample. Supported by National Institutes of Health grant RR01219 (C. Mannella, P.I.), through the National Center for Research Resources Biomedical Research Technology Program.

References

Alloyeau D, Hsieh WK, Anderson EH, Hilken L, Benner G, Meng X, Chen FR, Kisielowski C. Imaging of soft and hard materials using a Boersch phase plate in a transmission electron microscope. Ultramicroscopy. 2010; 110:563–570.

Badde H, Reimer L. Der einfluss einer streuenden phasenplatte auf das elektronenmikroskopische bild. Z. Naturforsch. 1970; 25:760–765.

Balossier G, Bonnet N. Use of an electrostatic phase plate in TEM. Transmission electron microscopy: improvement of phase and topographical contrast. Optik. 1981; 58:361–376.

Barton B, Joos F, Schröder R. Improved specimen reconstruction by Hilbert phase contrast tomography. J. Struct. Biol. 164:210–220. [PubMed: 18725304]

Boersch H. Über die kontraste von atomen in elektronenmikroskop. Z. Naturforsch. 1947; 2a:615–633.

Brink J, Gross H, Tittmann P, Sherman MB, Chiu W. Reduction of charging in protein electron cryomicroscopy. J. Microsc. 1998; 191:67–73. [PubMed: 9723190]

Cambie R, Downing K, Typke D, Glaeser R, Jin J. Design of a microfabricated, two-electrode phase-contrast element suitable for electron microscopy. Ultramicroscopy. 2007; 107:329–339. [PubMed: 17079082]

Chen F, Huang S, Shiue J, Hwu Y, Chang W, Kai J, Tseng F, Chang C. Development and application of Zernike electrostatic phase plate: practice and theory. Korean J. Microsc. 2008; 38(4)(Suppl.): 1273–1274.

Danev R, Nagayama K. Transmission electron microscopy with Zernike phase plate. Ultramicroscopy. 2001; 88:243–252. [PubMed: 11545320]

Danev R, Nagayama K. Single particle analysis based on Zernike phase contrast transmission electron microscopy. J. Struct. Biol. 2008; 161:211–218. [PubMed: 18082423]

Danev R, Glaeser R, Nagayama K. Practical factors affecting the performance of a thin-film phase plate for transmission electron microscopy. Ultramicroscopy. 2009; 109:312–325. [PubMed: 19157711]

Danev R, Kanamaru S, Marko M, Nagayama K. Zernike Phase Contrast Cryo-Electron Tomography. J. Struct. Biol. 2010; 171(2):174–181. [PubMed: 20350600]

Danev R, Nagayama K. Phase plates for transmission electron microscopy. Methods in Enzymology. 2010; 481:345–370.

Danov K, Danev R, Nagayama K. Electric charging of thin films measured using the contrast transfer function. Ultramicroscopy. 2001; 87:45–54. [PubMed: 11310540]

Downing KH, McCartney MR, Glaeser RM. Experimental characterization and mitigation of specimen charging on thin films with one conducting layer. Microsc. Microanal. 2004; 10:783–789. [PubMed: 19780320]

Faget, J.; Fagot, M.; Ferré, M.; Fert, C. Microscopie electronique a contraste de phase; Proc. 5th Intl. Cong. Electron Microsc.; Academic Press, New York. 1962; p. A-7-A-8.

Glaeser RM, Downing KH. Specimen charging on thin films with one conducting layer: discussion of physical principles. Microsc. Microanal. 2004; 10:790–796. [PubMed: 19780321]

Hoppe W. Use of zone correction plates and other techniques for structure determination of aperiodic objects at atomic resolution using a conventional electron microscope. Phil. Trans. Roy. Soc. Lond. B. 1971; 261:71–94.

Hosogi N, Shigematsu H, Terashima H, Homma M, Nagayama K. Zernike phase contrast cryo-electron tomography of sodium-driven flagellar 3 hook-basal bodies from Vibrio alginolyticus. J. Struct. Biol. 2010; 173:67–76. [PubMed: 20705140]

Hsieh C, Leith A, Mannella CA, Frank J, Marko M. Towards high-resolution three-dimensional imaging of native mammalian tissue: Electron tomography of frozen-hydrated rat liver sections. J. Struct. Biol. 2006; 153(1):1–13. [PubMed: 16343943]

Huang S, Wang W, Chang C, Hwu Y, Tseng F, Kai J, Chen F. The fabrication and application of Zernike electrostatic phase plate. J. Electron Microsc. 2006; 55:273–280.

Johnson H, Parsons D. Enhanced contrast in electron microscopy of unstained biological material, III. In-focus phase contrast of large objects. J. Microscopy. 1973; 98:1–17.

Kanaya K, Kawakatsu H, Ito K, Yotsumoto H. Experiment on the electron phase microscope. J. Appl. Phys. 1958; 29:1046–1049.

Kaneko Y, Danev R, Nagayama K, Nakamoto H. Intact carbocysome in a cyanobacterial cell visualized by Hilbert differential contrast transmission electron microscopy. J. Bacteriol. 2006; 188:805–808. [PubMed: 16385071]

Krakow W, Siegel B. Phase contrast in electron microscope images with an electrostatic phase plate. Optik. 1975; 42:245–268.

Majorovits E, Schröder R. Improved information recovery in phase contrast EM for non- two-fold summetric Boersch phase plate geometry. Microsc Microanal. 2002; 8s2:540CD.

Majorovits E, Barton B, Schultheiß K, Pérez-Willard F, Gerthsen D, Schröder R. Optimizing phase contrast in transmission electron microscopy with an electrostatic (Boersch) phase plate. Ultramicroscopy. 2007; 107:213–226. [PubMed: 16949755]

Majorovits E, Barton B, Benner G, Dietl C, Kühlbrandt W, Lengweiler S, Mandler T, Matijevic M, Niebel H, Schröder RR. Phase Contrast Aberration Corrected Electron Microscope for Phase Plate Imaging. Microsc. Microanal. 2010; 16(Suppl 2):534–535.

Malac M, Beleggia M, Egerton R, Zhub Y. Imaging of radiation sensitive samples in transmission electron microscopes equipped with Zernike phase plates. Ultramicroscopy. 2007; 108:126–140. [PubMed: 17509765]

Malac M, Kawasaki M, Beleggia M, Li P, Egerton R. Convenient contrast enhancement by hole free phase plate in a TEM. Microsc. Microanal. 2010; 16(Suppl 2):526–527.

Marko M, Hsieh C, Dunn K, Typke D, Mannella CA, Frank J. Use of the Zernike phase plate for electron tomography of frozen-hydrated specimens. Microsc. Microanal. 2005; 11(Suppl 2): 310CD.

Marko M, Hsieh C-E, Dunn KA, Typke D, Mannella CA, Frank J. Use of the Zernike phase plate for electron tomography of frozen-hydrated specimens. Microsc. Microanal. 2005; 11(Suppl 2): 310CD.

Marko M. “Universal” Phase-Plate Imaging for Cryo-Electron Tomography. Microsc. Microanal. 2007; 12(Suppl 2):1212. CD.

Marko M, Hsieh C, Leith A, Mannella C. Requirements for Phase-Plate Cryo-Electron Tomography. Microsc. Microanal. 2010; 15(Suppl 2):576–577.

Mastronarde D. Automated electron microscope tomography using robust prediction of specimen movements. J. Struct. Biol. 2005; 152:36–51. [PubMed: 16182563]

Matsumoto T, Tonomura A. The phase constancy of electron waves traveling through Boersch’s electrostatic phase plate. Ultramicroscopy. 1996; 63:5–10.

Möllenstedt, G.; Speidel, R.; Hoppe, W.; Langer, R.; Katerbau, K-H.; Thon, F. In: Bocciarelli, DS., editor. Electron microscopical imaging using zonal correction plates; Proc 4th European Regional Conference on Electron Microsc.; Tipografia Poliglotta Vatacana, Roma. 1968; p. 125-126.

Moretz R, Johnson H, Parsons D. Thickness estimation of carbon films by electron microscopy of transverse sections and optical density measurements. J. Appl. Phys. 1968; 39:5421–5426.

Motoki S, Fukuda T, Suga H, Okura Y, Danev R, Brink J, Armbruster B. Design evolution of the Zernike phase contrast transmission electron microscope. Microsc. Microanal. 2010; 16(Suppl 2): 530–531.

Müller, H.; Jin, J.; Danev, R.; Spence, J.; Padmore, H.; Glaeser, R. Design of an electron microscope phase plate using a focused continuous-wave laser. 2010. http://arxiv.org/abs/1002.4237v1

Murata K, Liu X, Danev R, Jakana J, Schmid MF, King JA, Nagayama K, Chiu W. Zernike phase contrast cryo-electron microscopy and tomography for structure determination at nanometer and sub-nanometer resolutions. Structure. 2010; 18:903–912. [PubMed: 20696391]

Nagayama K. A novel phase-contrast transmission electron microscopy producing high-contrast topographic images of weak objects. J. Biol. Phys. 2002; 28:627–635.

Nagayama K, Danev R. Phase contrast electron microscopy: development of thin-film phase plates and biological applications. Phil. Trans. R. Soc. B. 2008; 363:2153–2162. [PubMed: 18339604]

Nagayama K, Danev R, Okawara H, Yamamoto K, Hirayama T, Kitayama A. An Aharonov-Bohm effect design for Hilbert differential phase contrast. Korean J. Microsc. 2008; 38(4)(Suppl.):1276–1277.

Schröder R, Barton B, Rose H, Benner G. Contrast enhancement by anamorphotic phase plates in an aberration corrected TEM. Microsc. Microanal. 2007; 13s2:136–137.

Setou M, Danev R, Atsuzawa K, Yao I, Fukuda Y, Usuda Y, Nagayama K. Mammalian cell nano-structures visualized by cryo Hilbert differential contrast transmission electron microscopy. Med. Mol. Morphol. 2006; 39:176–180. [PubMed: 17187178]

Shigematsu H, Sokabe T, Danev R, Tominaga M, Naagayama K. A 3.5-nm structure of rat TRPV4 cation channel revealed by Zernike phase-contrast cryoelectron microscopy. J. Biol. Chem. 2010; 285:11210–11218. [PubMed: 20044482]

Shiue J, Chang C-S, Huang S-H, Hsu C-H, Tsai J-S, Chang W-H, Wu Y-M, Lin Y-C, Kuo P-C, Huang Y-S, Hwu Y, Kai JJ, Tseng F-G, Chen F-R. Phase TEM for biological imaging utilizing a Boersch electrostatic phase plate: theory and practice. J. Electr. Microsc. 2009; 58(3):137–145.

Shiue J, Hung S-K. A TEM phase plate loading system with loading monitoring and nano-positioning functions. Ultramicroscopy. 2010; 110:1238–1242. [PubMed: 20554117]

Suloway C, Pulokas J, Fellmann D, Cheng A, Guerra F, Quispe J, Stagg S, Potter C, Carragher B. Automated molecular microscopy: The new Leginon system. J. Struct. Biol. 2005; 151:41–60. [PubMed: 15890530]

Tochigi, H.; Nakatsuka, A.; Fukami, A.; Kanaya, K. In: Favard, P., editor. The improvement of the image contrast by using the phase plate in the transmission electro microscope; Proc 7th Internal. Cong. Electron Microsc., Grenoble; Société Française de Microscopie Electronique, Paris. 1970; p. 73-74.

Thon, F.; Willasch, D. In: Favard, P., editor. Hochauflösungs-elektronenmikroscopie mit Spezialaperturblenden und Phasenplatten; Proc 7th Internal. Cong. Electron Microsc., Grenoble; Société Française de Microscopie Electronique, Paris. 1970; p. 3-4.

Unwin P. Phase contrast and interference microscopy with the electron microscope. Phil. Trans. Roy. Soc. Lond. B. 1971; 261:95–104. [PubMed: 4399209]

Unwin P. Phase contrast electron microscopy of biological materials. J. Microsc. 1973; 98:299–312. [PubMed: 4126993]

Yamaguchi M, Danev R, Nishiyama K, Sugawara K, Nagayama K. Zernike phase contrast electron microscopy of ice-embedded influenza A virus. J. Struct. Biol. 2008; 162:271–276. [PubMed: 18313941]

Zhang J, Nakamura N, Shimizu Y, Liang N, Liu X, Jakana J, Marsh M, Booth C, Shinkawa T, Nakata M, Chiu W. JADAS: a customizable automated data acquisition system and its application to ice-embedded single particles. J. Struct. Biol. 2009; 165(1):1–9. [PubMed: 18926912]

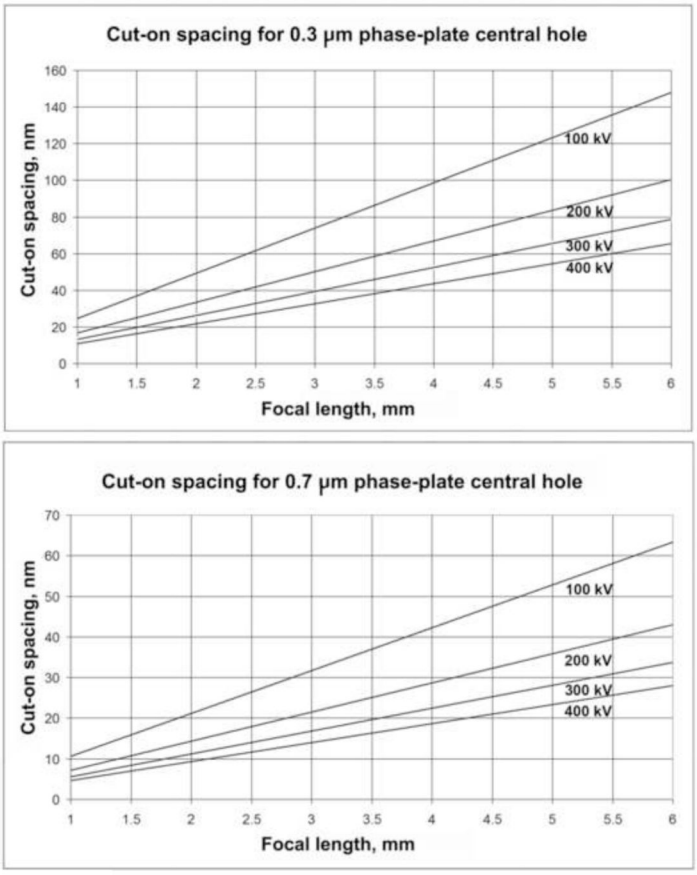

Figure 1.

Cut-on spacings for a 0.3-μm-diameter phase-plate central hole, the typical minimum size for an FEG TEM, and a 0.7-μm phase-plate central hole, the typical minimum size for a LaB_6 TEM. Plots are shown at 100, 200, 300, and 400 kV as a function of objective lens focal length.

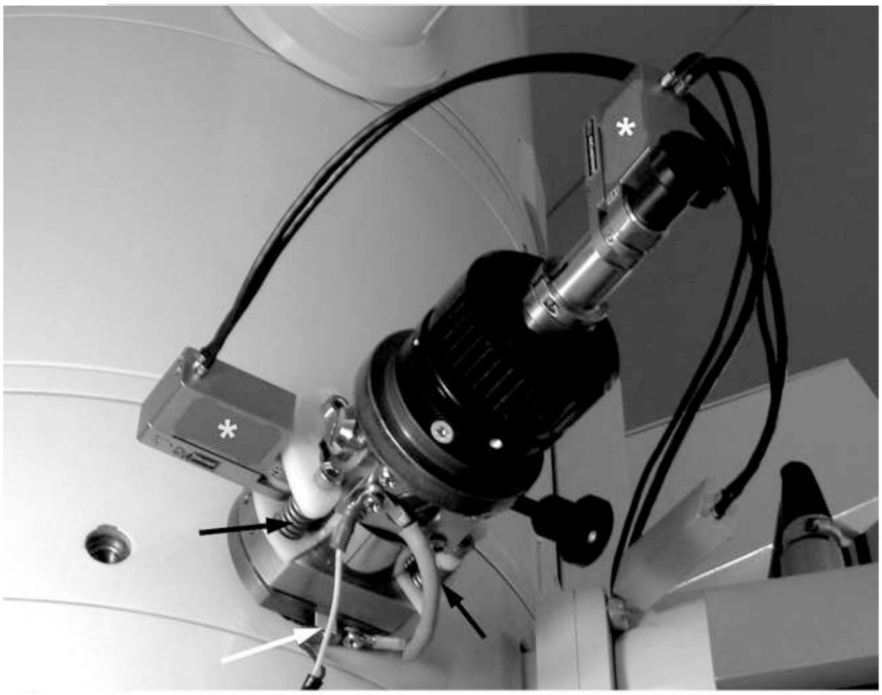

Figure 2.
Modified objective aperture drive on a JEOL JEM-4000FX TEM. Note piezo drivers (*), plastic pivot (white arrow), and springs (black arrows).

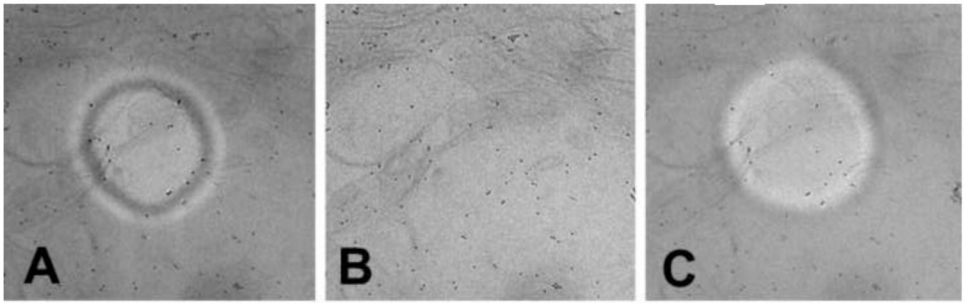

Figure 3.

Appearance of phase-plate central hole when adjusting the final condenser lens for the "on-plane" condition. (A) Condenser lens too weak, (B) proper setting of condenser lens, (C) condenser lens too strong. With our LaB_6 TEM, we find that the setting in (C) gives better contrast for centering the phase plate. With an FEG TEM, many fringes can be seen inside the off-plane phase-plate central hole.

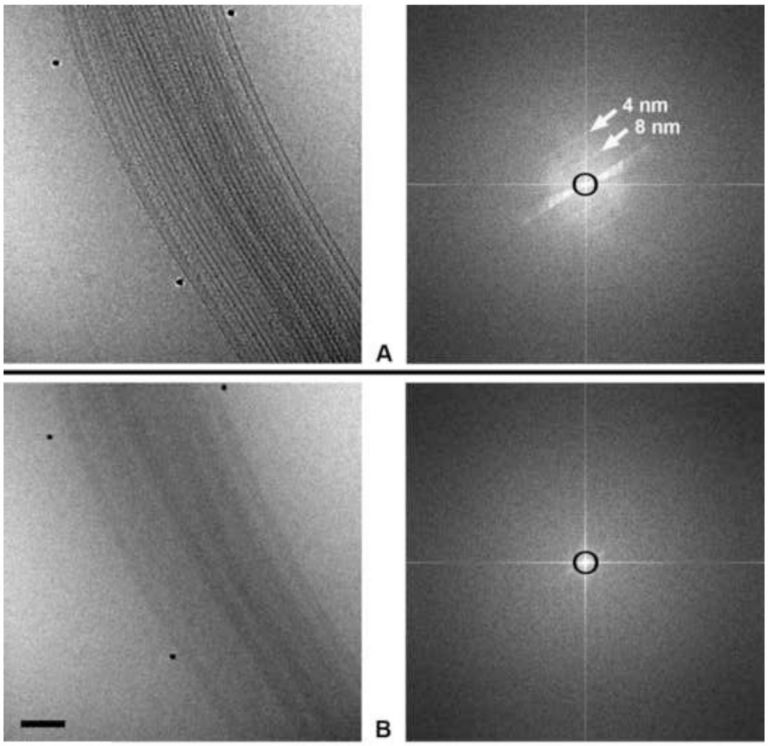

Figure 4.

Images (left) and corresponding power spectra (right) of a sea urchin axoneme membrane removed) recorded at 400 kV with zero-loss energy filtering, using a pixel size on the specimen of 0.5 nm and a CCD-image with a Nyquist-frequency spacing of 1 nm. (A) In-focus image using a phase plate with a cut-on spacing of 16 nm (represented by the black circles on the power spectra). Layer lines corresponding to helical spacings of 4 and 8 nm are indicated by arrows. As planned, the information falls off close to the CCD camera Nyquist frequency. We recommend a pixel size about one-quarter of the target resolution; using a phase plate, the focus should be adjusted so that the intensity fall-off in the power spectrum is beyond the half-Nyquist frequency of the CCD image (i.e 4 nm in this case). (B) The same field recorded in-focus but without phase plate, showing the same falloff in intensity, but far less contrast. Bar = 100 nm.

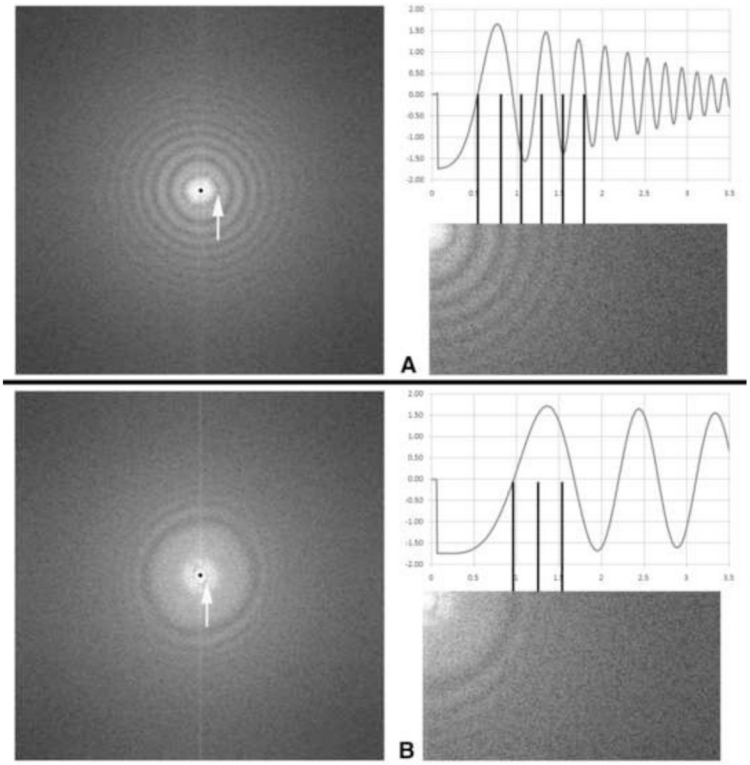

Figure 5.

Power spectra and calculated CTF plots of a phase plate that has acquired a charge. (A) Nominal underfocus 2 μm. The CTF minimum indicated by the arrow is characteristic of charging, and does not appear in a calculated CTF. The first "true" zero would indicate an underfocus of 1 μm, but note that the subsequent zeros are evenly-spaced, and do not correspond to a normal phase-plate CTF at 1 μm underfocus. This is another characteristic of charging (Danov et al., 2001). (B) The same phase plate with an applied overfocus of 3 μm relative to in-focus as determined by beam-tilt (e.g. the image wobbler). Again, the minimum close to the origin is a charging artifact. The first "true" CTF zero corresponds to an overfocus of 350 nm. Note that nevertheless there is strong contrast transfer to a spatial frequency of 0.5 nm^{-1}, corresponding to a spacing of 2 nm. Thus, after using defocus to compensate for charging, this phase plate would be useable for moderate-resolution imaging. Images recorded at 400 kV with 0.14 nm pixel size; phase-plate cut-on frequency 16 nm (represented by tiny dots in the left-hand images), convergence angle about 0.5 mrad.

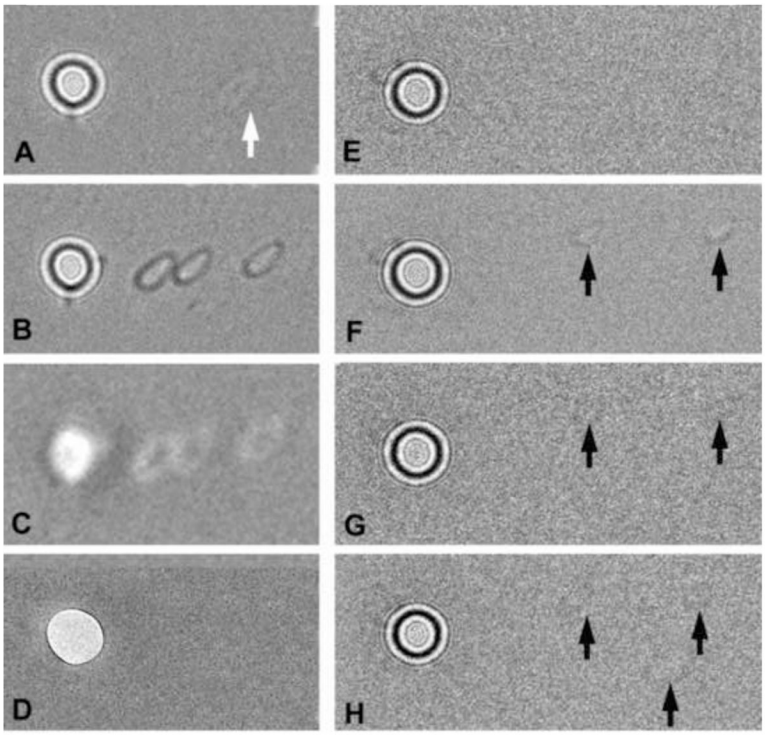

Figure 6.

Testing charge of phase-plate carbon films. Appearance of two phase plates (A-D and E-H) after spot-irradiation of the carbon film adjacent to the central hole. No specimen is inserted, and the condenser lens is set for the on-plane condition, with a total beam current of 1 nA. After spot irradiation, the condenser is overfocused, and images are recorded with an electron dose of 0.24 e^{-}/nm^2 on the carbon film. (A) Phase plate after spot-irradiation (at arrow) with 3×10^6 e^{-}/nm^2. This corresponds to an incident electron dose on the specimen (if it were present) of 150 e^{-}/nm^2. The faint white footprint indicates neutralization of positive charge on the carbon film, as typified by the Berriman effect. Note that the beam footprint, while small enough to pass the central hole, is not round (due to slight condenser-lens astigmatism), in spite of the fact that the illumination appeared circular at the specimen plane. (B,C) Demonstration of contrast reversal when the condenser lens is underfocused with respect to the on-plane condition. (D) In-focus image of the phase plate taken in the "low-mag" mode, focused by the objective minilens. The footprints are not visible, indicating that they are not due to appreciable contamination (which would be detectable by amplitude contrast). (E) Phase plate before spot irradiation. (F) Two footprints (arrows) created from individual spot exposures of 6×10^6 e^{-}/nm^2. Image recorded with double intensity to make the footprints more visible. (G) Image of phase plate after the entire phase plate was illuminated with a strong beam for 15 min (total dose 2.8×10^{15} $e^{-}/\mu m^2$). The footprints are nearly erased due to a charge neutralization effect and/or etching of most of the insulating contamination on the phase plate. (H) A third, slightly larger, footprint was created (lower arrow). Since the phase plate is now less-charged, the new footprint is fainter than in (F). The amount of charging of both of these phase plates was not excessive for medium-resolution imaging, and they yielded images with good phase contrast.

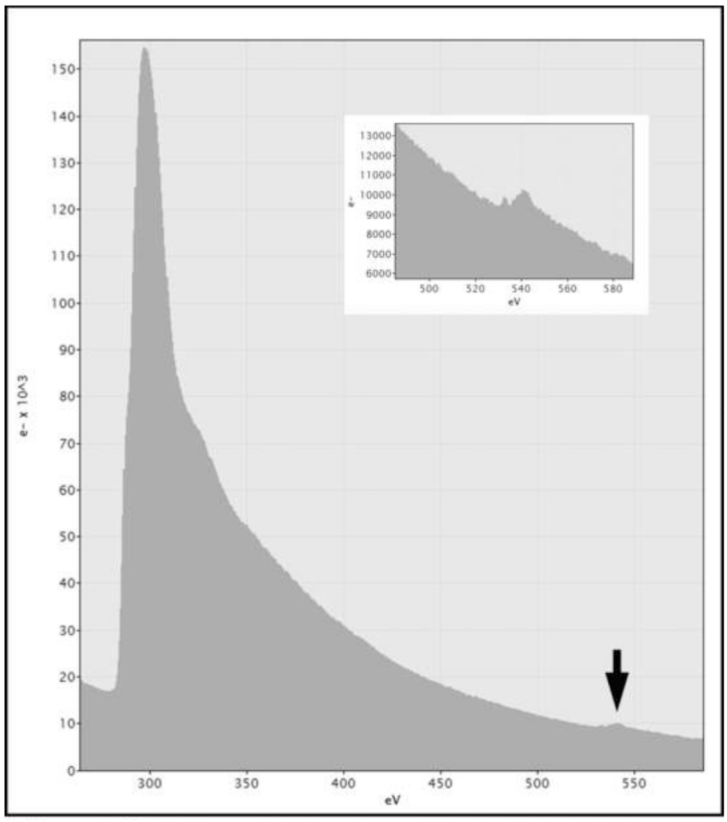

Figure 7.
EELS spectrum of the phase plate shown in Fig. 6A-D. Note the small oxygen edge at the arrow and in the inset, indicating some contamination. This phase plate had been in the TEM for two months, during which time the phase plate was used rarely, but general imaging of frozen-hydrated specimens was done nearly daily.

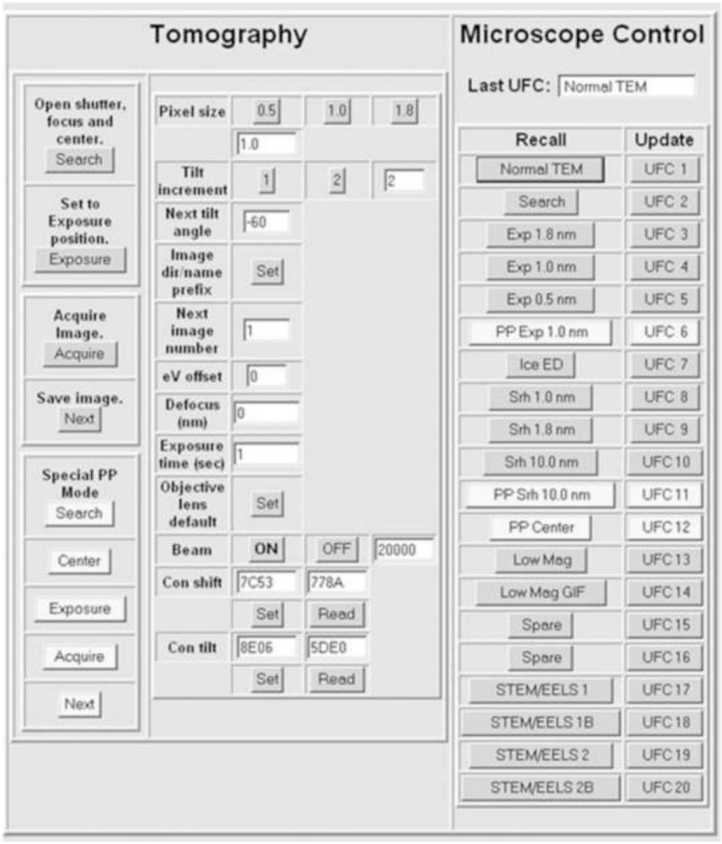

Figure 8.

Graphical user interface for the Albany JEM-4000FX. The buttons used for phase-plate imaging are in a lighter shade. Under Microscope Control (right-hand-side panel), various TEM setups are stored in the “user function conditions” of the EM internal computer, for instant storage and recall. Some of these are for the buttons on the left-side panel. Under Tomography (left-hand side), the upper four buttons are used for collecting non-phase-plate tilt series. The lower buttons include one for setting the “off-plane” condition, needed for centering the phase plate. The “eV offset” field provides compensation for possible drift of the zero-loss peak when using the energy filter. The “Defocus” field allows for offset of focus between “wobbler focus” and the defocus compensation needed because of mild charging of the phase plate (or is used to set the desired underfocus for non-phase-plate imaging). Beam ON and OFF is used to apply the amount of deflection, entered at the right, when the beam is blanked. The beam ON button can be activated by a footswitch connected to the microswitch in the mouse. The “Objective lens default” button sets the focus value for the goniometer eucentric point. The “Con shift” and “Con tilt” buttons are used to set the starting conditions at the beginning of data collection, and to recover them should the phase plate jump far off position and need mechanical re-centering. The Tomography functions can be used for collecting a series of un-tilted images simply entering zero as the next tilt angle.

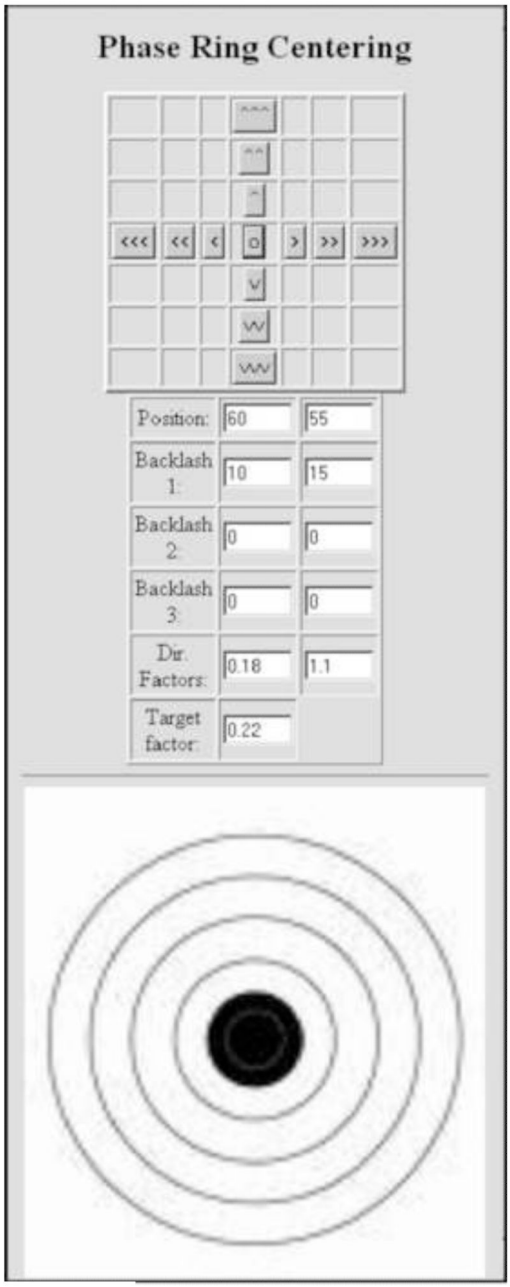

Figure 9.
Phase-plate centering interface used at Albany. The upper panel moves the phase plate in orthogonal directions with a choice of three step sizes; the center button resets the piezo drivers to the center of travel. The position boxes show the applied voltages. Three backlash values can be entered to compensate for mechanical linkages, piezo drift, and piezo hysteresis. Directional factors adapt the movement so that it is orthogonal relative to the image on the CCD camera. The target factor compensates for the different mechanical advantages of the two drive arrangements.

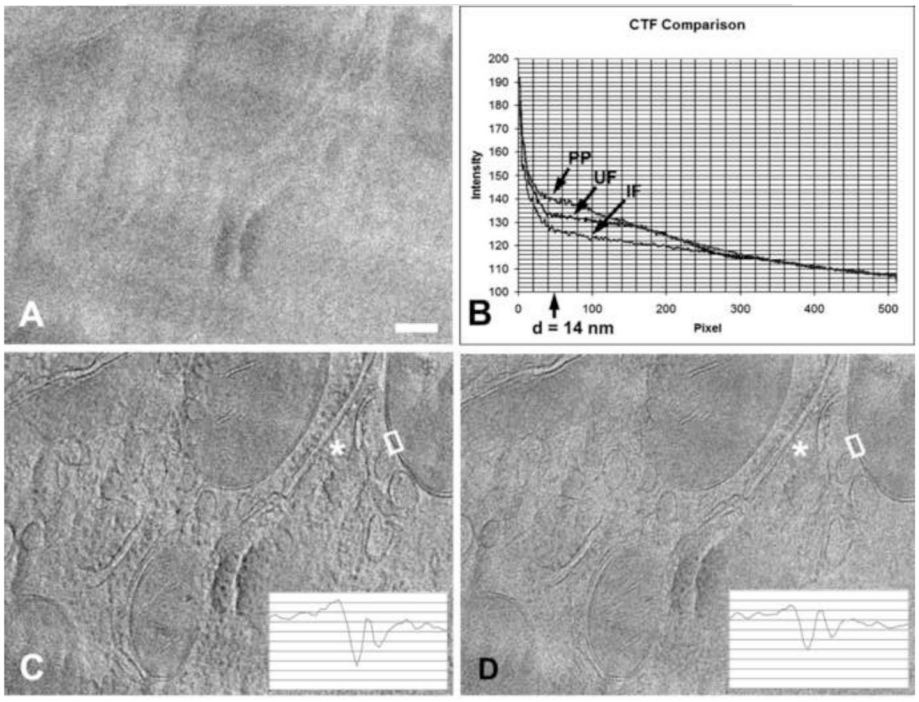

Figure 10.

Comparison of in-focus phase plate imaging and conventional high-underfocus imaging without phase plate. (A) Near-focus image without phase plate of a 200-nm-thick vitreously frozen cryo-ultramicrotome section of rat liver tissue. (B) Rotationally averaged power spectra of images A (IF), C (PP) and D (UF). The phase-plate cut-on spacing of 14 nm is indicated. Note improved low-frequency transfer with phase-plate imaging. (C) Near-focus image using a phase plate. (D) Image taken at 20 μm underfocus (corresponding to a spacing of 5.5 nm) without phase plate. Insets in C and D show traces across mitochondrial membranes within the white boxes on the images. Note the improved visibility of ribosomes on the endoplasmic reticulum at (*). Images recorded at 400 kV with zero-loss energy filtering. Bar = 100 nm.